Supporting Information (SI) for *ACS Nano*

In-Situ Fabrication of 3D Ag@ZnO Nanostructures for Microfluidic Surface-Enhanced Raman Scattering Systems

Yuliang Xie,[1,2,‡] Shikuan Yang,[1,‡] Zhangming Mao,[1] Peng Li,[1] Chenglong Zhao,[1] Zane Cohick,[1] Po-Hsun Huang,[1] and Tony Jun Huang[1,2]*

[1] Department of Engineering Science and Mechanics, The Pennsylvania State University, University Park, PA 16802, USA

[2] Department of Chemical Engineering, The Pennsylvania State University, University Park, PA 16802, USA

‡ These authors contributed equally

** Address correspondence to junhuang@psu.edu*

Estimation of Laser Energy Input. The absorbed laser energy was calculated from the total incidence laser energy, the coefficients of transmission and reflection of the gold-coated glass slides. The total incidence laser power was measured by a power meter (FieldMaxII-TO, Coherent, USA) after the objective lens. The measured power was about 15 mW for ZnO nanorod fabrication. The transmission and reflection coefficients of the gold-coated glass slides was measured by a UV/Vis spectrometer (Lambda 950, PerkinElmer, USA), which were 0.12 and 0.3, respectively. The upper-limit of the power absorbed by the gold film (P_a) was estimated as:

$$P_a=P_{in}-P_r-P_t,$$

where P_{in} is the total incidence laser power, P_r is the reflected power, and P_t is the transmitted power. Therefore, P_a was calculated as 8.7 mW and was used in the simulation as the heat rate.

On-chip Surface-Enhanced Raman Scattering (SERS) Detections of Proteins and DNAs. The ability to probe organic molecules such as proteins and DNAs is very important in environmental protection and medical diagnostics. As proof of concepts, BSA (0.01 %, w/w) and DNA (1 μM) were used to evaluate the SERS performance of the 3D Ag@ZnO nanorods. The SERS peak positions of BSA (Fig. S1a) are in good agreement with those previously reported.[1] Briefly, the 845 cm^{-1} SERS peak is from the tyrosine group; the peaks located at 940 cm^{-1} are from the skeletal stretching of α-helix; the C-N bond vibration in the protein structure gave rise to the appearance of the 1112 cm^{-1} peak; the peak at 1265 cm^{-1} is originated from the Amide III; and the

peaks at 1362 cm^{-1} and 1434 cm^{-1} can be assigned to the vibrations of the CH, CH_2, and CH_3 groups in the proteins.

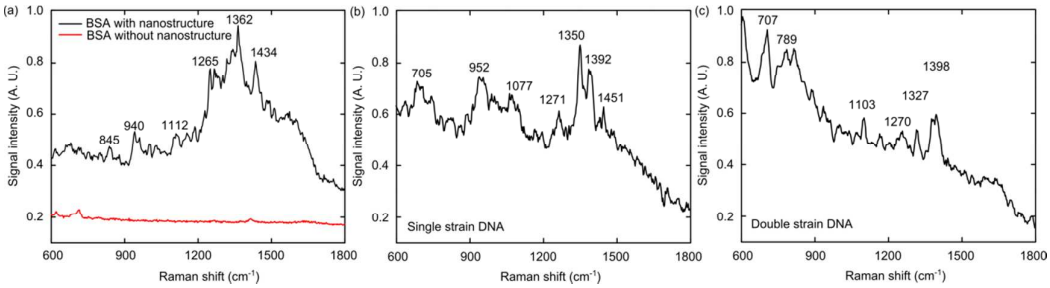

Figure S1. SERS spectra of (a) BSA, (b) single-stranded DNA, and (c) double-stranded DNA absorbed on the 3D Ag@ZnO SERS substrates.

Label-free SERS detection of single-stranded DNA (ssDNA) and its hybridization product, double-stranded DNA (dsDNA), were also explored (Fig. S1b, c). In this case, DNA hybridization of BRCA1 gene, known to cause breast and ovarian cancer, was detected in our system. In experiments, we prepared a ssDNA molecular beacon (MB) and its complementary ssDNA. The ssDNA MB was first injected in the channel with 1 μM concentration and its SERS spectrum was detected. The SERS peaks from ssDNA MB (Fig. 6c) could be attributed to the backbone (952 cm^{-1} is from deoxyribose phosphate backbone; 1450 cm^{-1} is from the deformation of CH_2 in the DNA backbone) or the A (705 cm^{-1}), T (1350 cm^{-1}), G (1350 cm^{-1} and 1392 cm^{-1}), and C (1271 cm^{-1}), as previously reported.[2,3] After hybridization with the complimentary strand, several interesting features were observed in the SERS spectrum of the dsDNA. First, the overall intensity of the SERS peaks decreased even under the same experimental conditions. In addition, several SERS peaks disappeared,

others shifted, and some new peaks emerged (Fig. 6d). We believe this evolution of the SERS peaks is induced by the structural change that follows hybridization. The exposed deoxynucleotide groups in the ssDNA were densely packed in their hybridized dsDNA preventing them from contacting the SERS hotspot. After hybridization, new bonds were formed, so the vibrational peak shifted slightly due to the changed environments. On the whole, the 3D Ag@ZnO SERS substrates developed here can distinguish the structural change of DNA in a liquid phase during the hybridization process; the substrates thereby have the potential to be used in gene diagnostics.

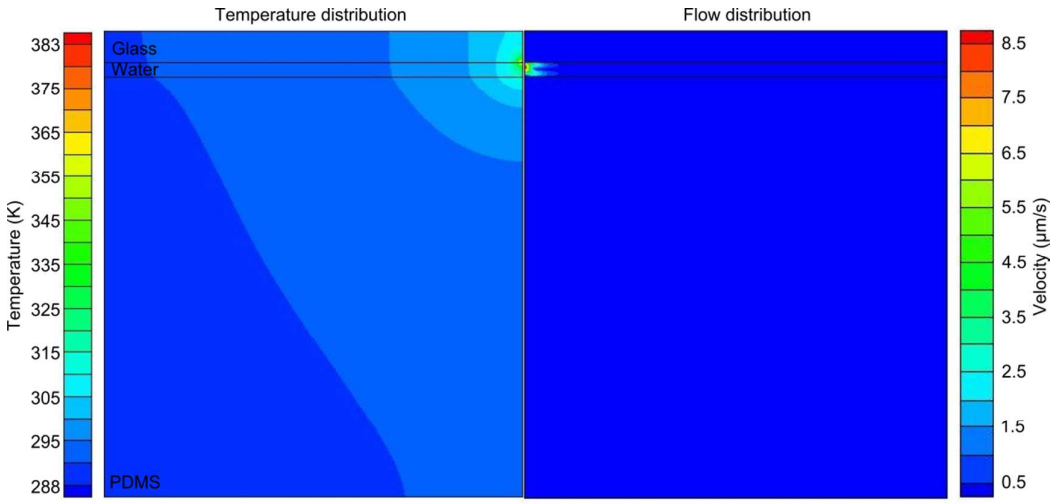

Figure S2. Temperature and flow distribution in the glass slides, liquids in the microfluidic channels, and the PDMS device.

More Simulation Results of Temperature and Flow Fields. In the simulation described in the main text, the thicknesses of the glass, liquid, and PDMS layers were 150 μm, 130 μm, and 2 mm, respectively. The width of the three layers was 2 mm.

Due to the sharp spatial distribution of temperature and flow, only simulation results near the laser spot were shown in the main text. Here Fig. S2 shows the result of the entire region.

Reference:

(1) Lin, V. J.; Koenig, J. L. Raman Studies of Bovine Serum Albumin. *Biopolymers* **1976**, *15*, 203–218.

(2) Prescott, B.; Steinmetz, W.; Thomas, G. J. Characterization of DNA Structures by Laser Raman Spectroscopy. *Biopolymers* **1984**, *23*, 235–256.

(3) Barhoumi, A.; Zhang, D.; Tam, F.; Halas, N. J. Surface-Enhanced Raman Spectroscopy of DNA. *J. Am. Chem. Soc.* **2008**, *130*, 5523–5529.